

GmAKT1-mediated K⁺ absorption positively modulates soybean salt tolerance by GmCBL9-GmCIPK6 complex

Chen Feng[†], Muhammad Azhar Hussain[†], Yan Zhao, Yuning Wang, Yuyan Song, Yaxin Li, Hongtao Gao, Yan Jing, Keheng Xu, Wenping Zhang, Yonggang Zhou* and Haiyan Li* 

School of Breeding and Multiplication (Sanya Institute of Breeding and Multiplication), Hainan University, Sanya, 572025, Hainan, China

Received 4 November 2024;

revised 20 January 2025;

accepted 15 February 2025.

*Correspondence (Tel +86 13944885658;

fax +86 0898-31883115; email hyli@hainanu.edu.cn (H.L.); Tel +86

18543440015; fax +86 0898-31883115;

email ygzhou@hainanu.edu.cn (Y.Z.))

†These authors have made equal

contributions equally to this work.

Summary

Soybean is one of the most important crops in the world. However, salt stress poses a major challenge to soybean growth and productivity. Therefore, unravelling the complex mechanisms governing salt tolerance in soybean is imperative for molecular breeding of salt-tolerant varieties to improve yield. Maintaining intracellular Na⁺/K⁺ homeostasis is one of the key factors for plant salt tolerance. Although some salt tolerance mechanisms involving Na⁺ exclusion have been well identified in plants, few studies have been conducted on how K⁺ influx controls soybean salt tolerance. Here, we characterized the function of soybean K⁺ channel gene *GmAKT1* and identified GmCBL9-GmCIPK6 complex, which modulated GmAKT1-mediated K⁺ uptake under salt stress. Functional studies found that soybean lines *GmAKT1* overexpressing increased K⁺ content and promoted salt tolerance, while CRISPR/Cas9-mediated disruption of *GmAKT1* soybean lines decreased the K⁺ content and showed salt sensitivity. Furthermore, we identified that GmCIPK6 interacted with GmAKT1 and GmCBL9 interacted with GmCIPK6. In addition, Mn²⁺-Phos-tag assays proved that GmCIPK6 could phosphorylate GmAKT1. This collaborative activation of the GmCBL9-GmCIPK6-GmAKT1 module promoted K⁺ influx and enhanced soybean salt tolerance. Our findings reveal a new molecular mechanism in soybeans under salt stress and provide insights for cultivating new salt-tolerant soybean varieties by molecular breeding.

Keywords: Soybean, Salt stress, GmAKT1, GmCIPK6, GmCBL9.

Introduction

Soil salinization is one of the major abiotic stresses that adversely affect plant growth and development, resulting in significant losses in crop production worldwide (Liang *et al.*, 2024). Approximately 20%–30% of the world's 230 million hectares of arable land is undergoing soil salinization, and this circumstance will continue to worsen due to human activities and other climate change-related factors (Ismail and Horie, 2017). Furthermore, it is presumed that the global population will reach 9.7 billion by 2050, which will cause a 60% increase in food consumption compared to current levels (Bailey-Serres *et al.*, 2019; Hickey *et al.*, 2019). Hence, improving crop yield is necessary to meet food supply demands. Soybean (*Glycine max* L. Merr.) is an important legume crop that provides a large source of oil and protein for human diets and animal feed (Bian *et al.*, 2020), while soybean is classified as a moderately salt-tolerant crop, its yield will be reduced when salt concentrations exceed 5 dS/m (Phang *et al.*, 2008). Therefore, breeding more salt-tolerant soybeans will be an adaptive strategy to increase soybean yield on salinized agricultural land.

Salt stress affects plant physiological processes, including ionic, osmotic and oxidative stresses (Yang and Guo, 2018). Excessive Na⁺ accumulation disrupts K⁺ acquisition and distribution, resulting in impairment of cell metabolic processes (Rubio *et al.*, 2019; Van Zelm *et al.*, 2020). Hence, maintaining cytosolic Na⁺/K⁺ homeostasis is a key feature of salt tolerance in plants (Zhu, 2002). Notably, increased K⁺ uptake and translocation in plant tissues can limit Na⁺ absorption during salt stress

(Alvarez-Aragon *et al.*, 2016; Wu *et al.*, 2018). Thus, facilitating K⁺ uptake or reducing K⁺ efflux can effectively improve plant salt tolerance (Cao *et al.*, 2019; Roy *et al.*, 2014; Shen *et al.*, 2015).

K⁺ is an essential macroelement in plant cells, playing crucial roles in osmoregulation, enzyme activation, protein synthesis and membrane transport (Li *et al.*, 2018). A series of membrane channels and transporters are involved in K⁺ uptake in roots and its distribution throughout the plant (Nieves-Cordones *et al.*, 2023; Pantoja, 2021). The Arabidopsis K⁺ transporter 1 (AKT1) is one of the principal systems for K⁺ absorption in plants, conferring tolerance to low K⁺ conditions in plants (Li *et al.*, 2014; Xu *et al.*, 2006). Additionally, some studies reported that AKT1-mediated K⁺ absorption is related to salt tolerance in plants. In Arabidopsis, the deletion of *AKT1* showed root growth reduction and the decrease of K⁺ content in response to salt stress (Li *et al.*, 2023). The complementation of eggplant gene *SmAKT1* in Arabidopsis *akt1* mutants could enhance the salt tolerance of plants by keeping the Na⁺/K⁺ ratio (Li *et al.*, 2019). Similarly, expressing the *Puccinellia tenuiflora* gene *PutAKT1* in *akt1* mutants can increase the plant's K⁺ content and reduce Na⁺ accumulation under salt stress (Ardie *et al.*, 2010). Additionally, compared to wild-type *Zygophyllum xanthoxylum*, *ZxAKT1*-silenced plants decreased K⁺ concentrations and exhibited significant inhibition of plant growth in response to salt stress (Ma *et al.*, 2017). Although the AKT1-mediated salt tolerance regulatory network is well established in Arabidopsis and other crops, the underlying molecular mechanism of *GmAKT1*, specifically its upstream and downstream regulators for salt tolerance, remains fragmentary in soybeans.

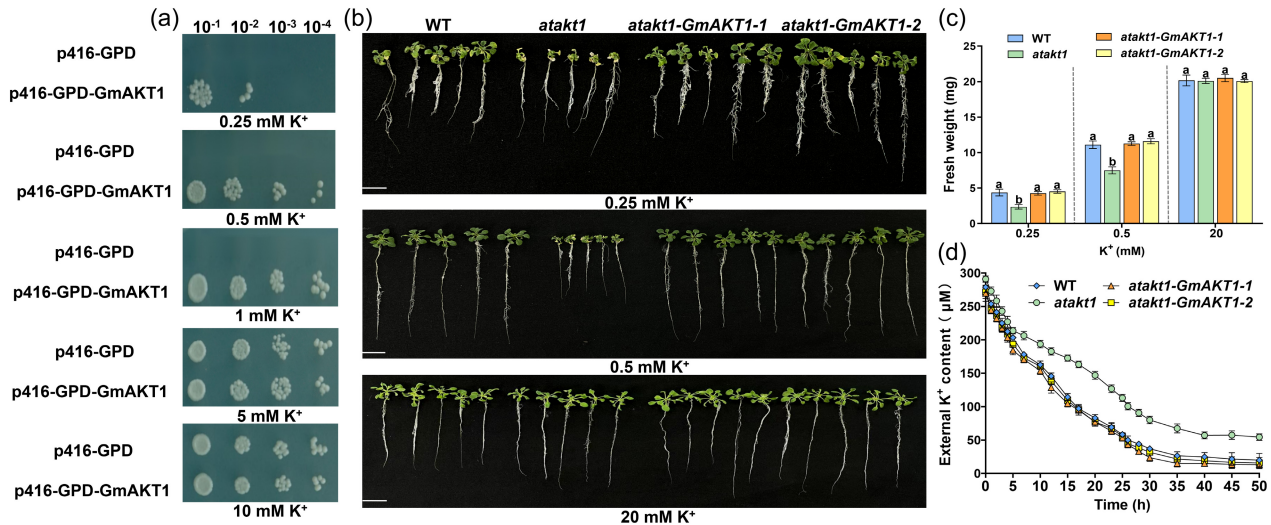


Figure 1 K⁺ uptake activity of GmAKT1 in yeast and Arabidopsis. (a) GmAKT1 improves the growth of K⁺ uptake-deficient yeast mutant R5421 on the AP medium containing different K⁺ concentrations. The transformation of pYES2 vector as negative control. *GmAKT1* was constructed into pYES2 vector and was transformed into yeast mutant R5421. The transgenic yeast cells were spotted in a 10-fold dilution series on the different K⁺ concentrations medium. (b) Phenotypic analysis of WT, *atakt1* mutant and Arabidopsis *atakt1*-complemented lines (*atakt1-GmAKT1-1* and *atakt1-GmAKT1-2*) under different K⁺ conditions for 16 days. (c) Fresh weight of WT, *atakt1* and two *atakt1*-complemented lines (*atakt1-GmAKT1-1* and *atakt1-GmAKT1-2*) under various K⁺ concentrations. Each bar is shown as mean \pm SD from $n = 12$ seedlings. Different letters indicate significant differences ($P < 0.05$, one-way ANOVA). (d) Kinetics of K⁺ uptake activity among WT, *atakt1* and two *atakt1*-complemented lines by the depletion of K⁺ assay. The data represent three independent experiments.

Calcineurin B-like proteins (CBLs) and CBL-interacting protein kinases (CIPKs) constitute an important signalling network for responding to salt stress. These proteins form CBL-CIPK complexes that target membrane transporters and channels, thereby controlling physiological processes in plants (Mao *et al.*, 2023; Tang *et al.*, 2020). In Arabidopsis, CBL4 (SOS3) interacts with CIPK24 (SOS2) to activate and phosphorylate Na⁺/H⁺ antiporter SOS1 (salt overly sensitive 1) under salt stress (Qiu *et al.*, 2002; Quintero *et al.*, 2011). Additionally, SOS1 can be activated by the CBL10-CIPK8 complex, which promotes Na⁺ extrusion and enhances salt tolerance (Yin *et al.*, 2020). Furthermore, calcium-permeable transporter Annexin4 is activated by the CBL10-CIPK24 complex in response to salt stress (Ma *et al.*, 2019). These studies demonstrate that the CBL-CIPK complexes are critical to modulating transporters in Arabidopsis under salt stress. Notably, some orthologues of the K⁺ channel gene *AKT1* have shown that AKT1-mediated K⁺ uptake is also regulated by CBLs and CIPKs in rice, maize and grape (Cuéllar *et al.*, 2013; Han *et al.*, 2021; Li *et al.*, 2014). However, it remains unknown whether GmCBL-GmCIPK complexes can regulate GmAKT1 and promote K⁺ uptake, thereby improving salt tolerance in soybeans.

In the previous study, we identified a soybean K⁺ channel gene *GmAKT1*, whose expression patterns were significantly upregulated in soybean roots and leaves under salt stress (Feng *et al.*, 2021). However, the function and mechanism for *GmAKT1* in response to salt stress remain to be further characterized. Here, we developed *GmAKT1* overexpression soybean lines and CRISPR/Cas9-mediated *GmAKT1* loss-of-function mutants to identify the role of *GmAKT1* in soybean under salt stress. Subsequently, we cloned *GmCBL* family genes and *GmCIPK* family genes and identified a regulatory network GmCBL9-

GmCIPK6-GmAKT1 by yeast two-hybrid (Y2G), bimolecular fluorescence complementation (BiFC) and Co-immunoprecipitation (Co-IP) experiments. On this basis, we reported that the GmCBL9-GmCIPK6 complex enhanced GmAKT1-mediated K⁺ uptake in yeast and patch-clamp whole-cell recording analysis. Finally, we demonstrated that coexpression of *GmCBL9* and *GmCIPK6* in *GmAKT1* overexpressing soybean lines could maintain cytoplasmic Na⁺/K⁺ balance and thus improve salt tolerance in soybean.

Results

GmAKT1 mediates K⁺-uptake activity in yeasts and Arabidopsis

To verify whether soybean *GmAKT1* possesses K⁺ uptake activity, we transformed *GmAKT1* into K⁺ uptake-deficient yeast mutant strain R5421(*trk1Δ*, *trk2Δ*). The results demonstrated that yeast mutant strain R5421 expressing *GmAKT1* could grow on AP (arginine-phosphate) medium containing K⁺ concentrations ranging from 0.25 to 10 mM (Figure 1a). However, yeast mutant strain R5421 could not grow under low K⁺ concentrations (below 5 mM K⁺). Furthermore, we transformed the coding sequence of *GmAKT1* into the Arabidopsis mutant *akt1* for ectopic overexpression and analysed the GmAKT1-mediated K⁺ activity in plants. Under normal condition (20 mM K⁺), the results showed that *akt1* mutant, WT (Col-0) and two complementary Arabidopsis lines (*akt1*, *akt1/GmAKT1-1* and *akt1/GmAKT1-2*) exhibited a similar phenotype and fresh weight (Figure 1b,c). Notably, compared with Arabidopsis mutant *akt1*, both complementary Arabidopsis lines and WT lines increased fresh weight under low K⁺ conditions (0.25 mM or 0.5 mM K⁺), suggesting that *GmAKT1* involved in low K⁺ stress and can enhance tolerance

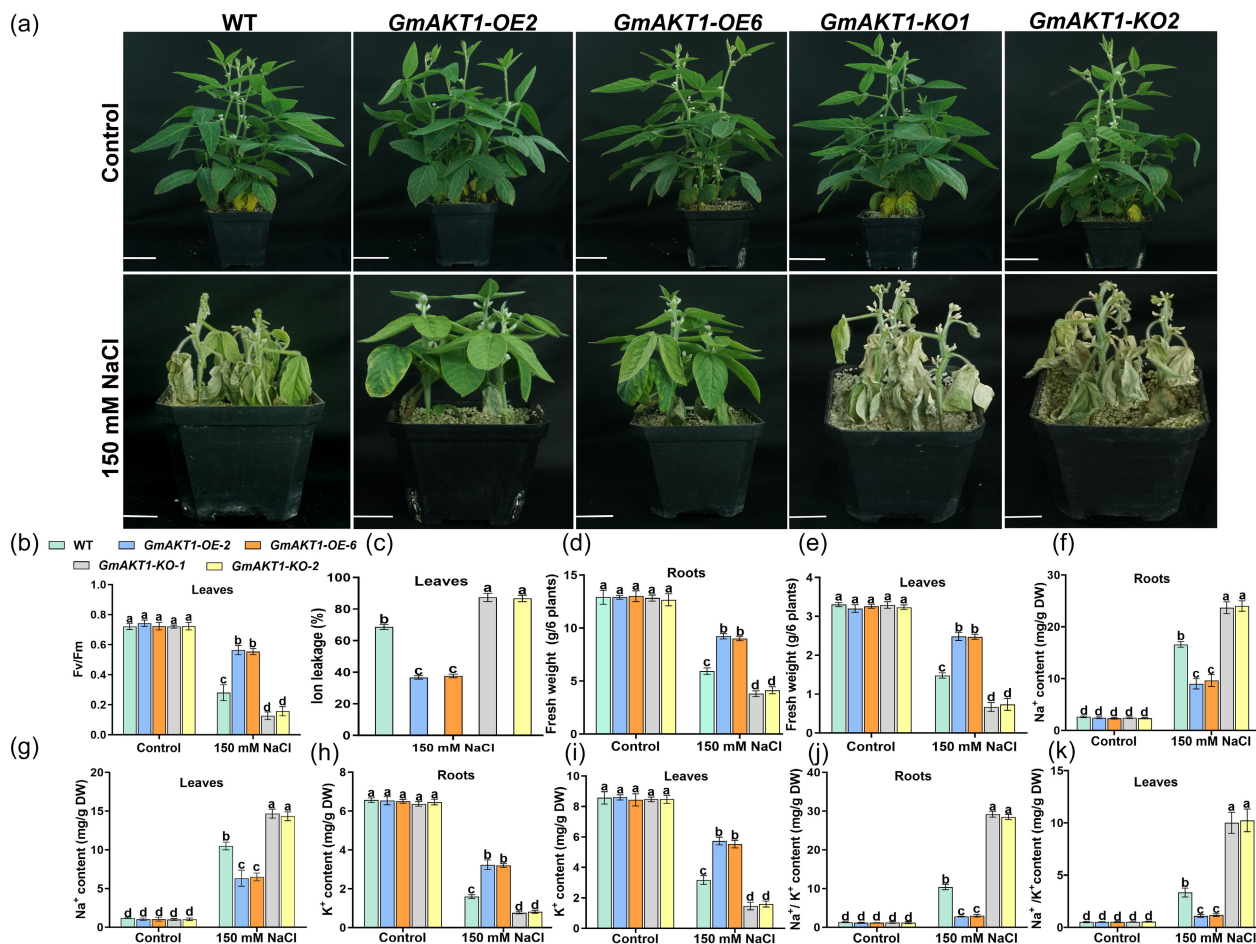


Figure 2 *GmAKT1* positively regulates salt resistance in soybean. (a) Phenotypic identification of different soybean lines (WT, *GmAKT1*-OE lines and *GmAKT1*-KO lines) under normal and salt stress (150 mM NaCl) for 32 days. Scale bar is 2 cm. (b–e) The representative photographs of soybean lines Fv/Fm in leaves (b), ion leakage from leaves (c), fresh weight of roots (d) and fresh weight of leaves (e). (f–k) The values of Na⁺ (f–g), K⁺ (h–i) and Na⁺/K⁺ ratio (j–k) of roots and leaves were shown in different soybean plants. For each assay, the data are shown as mean ± SD, *n* = three biologically independent experiments. Lowercase letters indicate significant differences between samples at *P* < 0.05, according to two-way ANOVA.

to low K⁺ stress (Figure 1b, c). Besides, in kinetic study of K⁺ depletion, the two complementary *Arabidopsis* lines exhibited more rapid depletion of external K⁺ compared to *Arabidopsis* mutant *akt1* (Figure 1d). Taken together, these results indicated that *GmAKT1* possesses K⁺ uptake activity under low K⁺ concentrations.

GmAKT1 positively regulates salt tolerance in soybean

To investigate whether *GmAKT1* has physiological roles in response to salt stress, we generated two homozygous T3 generation *GmAKT1*-overexpression (named *GmAKT1*-OE2 and *GmAKT1*-OE6) and two homozygous T3 generation CRISPR/Cas9-mediated loss-of-function mutants (named *GmAKT1*-KO1 and *GmAKT1*-KO2) transgenic soybean lines from 'Dong Nong 50' (DN50) background. RT-qPCR assays confirmed that *GmAKT1* transcript levels were higher in *GmAKT1*-OE lines than those in WT plants (Figure S1a). Additionally, DNA sequencing confirmed that a single base (A) was inserted or seven bases (TGGTTGT) were deleted at different PAM (protospacer adjacent sequences) sites in *GmAKT1*-KO lines, which

caused the conversions of amino acids that finally stopped encoding at 42 bp or 990 bp, respectively (Figure S1b,c).

For phenotypic assays, soybean seedlings at the V1 stage were treated with 150 mM NaCl for 23 days. Soybean leaves of WT and *GmAKT1*-KO showed more wilting than *GmAKT1*-OE lines under salt stress (Figure 2a). Furthermore, *GmAKT1*-OE lines exhibited higher fresh weight, Fv/Fm and lower ion leakage values than WT soybean plants in response to salt stress (Figure 2b–e). In contrast, *GmAKT1*-KO lines had lower fresh weight and Fv/Fm values than WT soybean plants under salt stress (Figure 2b–e). To further investigate whether *GmAKT1* can regulate ion balance, we measured Na⁺, K⁺ and Na⁺/K⁺ contents in soybean. Under normal growth condition, there were no significant differences in these ion contents between WT, *GmAKT1*-OE and *GmAKT1*-KO plants (Figure 2f–k). However, under salt stress, *GmAKT1*-OE lines had higher K⁺ and lower Na⁺ and Na⁺/K⁺ ratio compared to those of the WT and *GmAKT1*-KO lines (Figure 2f–k). Taken together, these results demonstrated that the overexpression of *GmAKT1* improved salt tolerance in soybean.

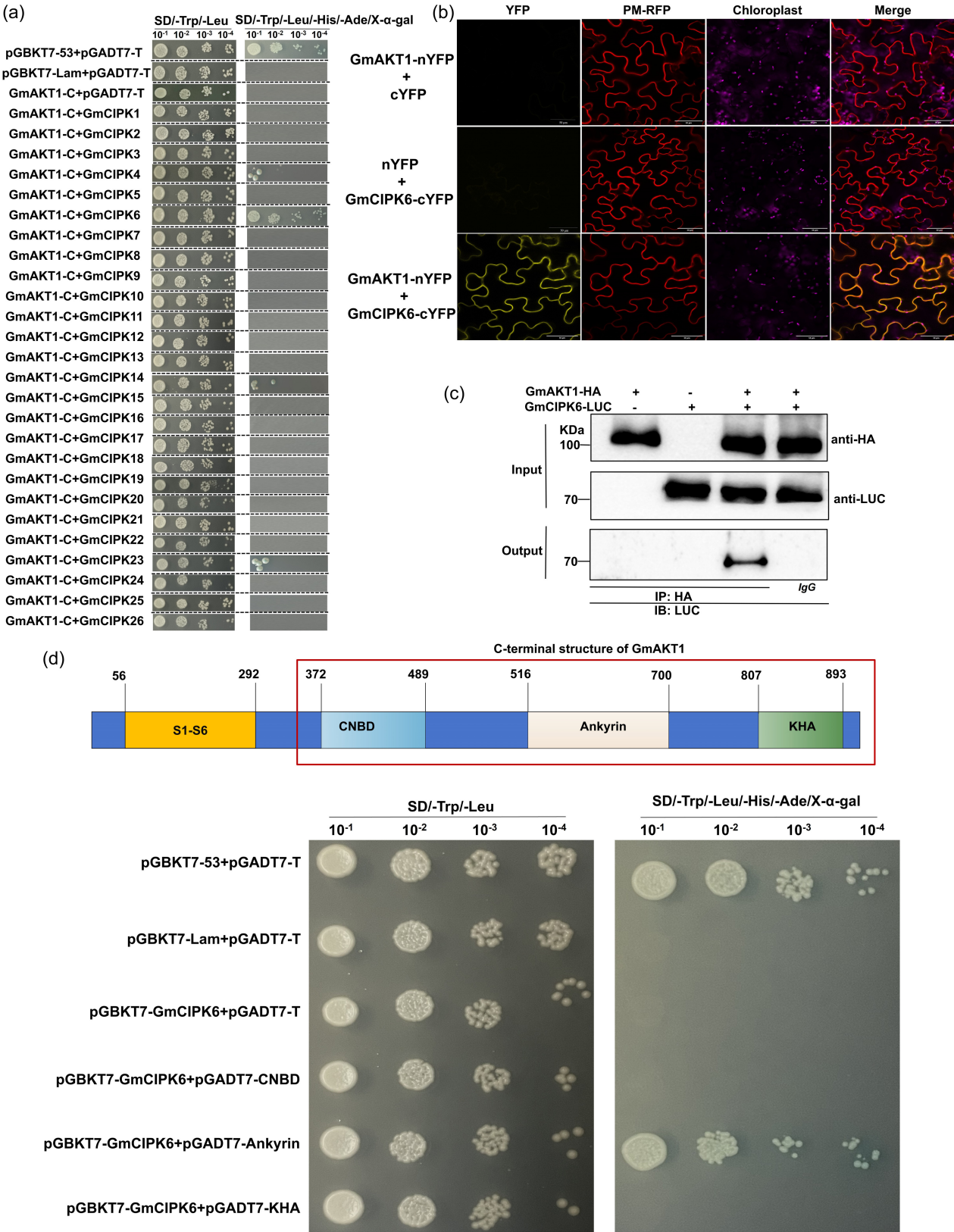


Figure 3 The interaction analysis between GmAKT1 and GmCIPK family members. (a) Yeast two-hybrid assays (Y2H) between the C-terminal part of GmAKT1 (GmAKT1-C) and the full length 26 GmCIPK family members. pGBKT7-53 + pGADT7-T serves as positive control, pGBKT7-Lam + pGADT7-T and GmAKT1-C + pGADT7-T represent negative control. The 1:10 serial dilutions of yeast cells were spotted on synthetic defined (SD) medium lacking Leu and Trp (SD-TL) or SD-Leu-Trp-His-Ade (SD-TLHA) with X- α -gal medium, respectively. (b) Bimolecular fluorescence complementation (BiFC) analysis for GmAKT1 and GmCIPK6 interaction in tobacco leaves. The YFP fluorescence was obtained by confocal microscopy. GmAKT1-nYFP+cYFP and nYFP+GmCIPK6-cYFP as negative control and GmAKT1-nYFP+GmCIPK6-cYFP as interaction proteins. PM-RFP as a cell membrane marker. Scale bar is 50 μ M. (c) Co-IP assays showing that GmAKT1 interacts with GmCIPK6. Co-IP assay showing that GmAKT1 interacts with GmCIPK6 in tobacco leaves. Total proteins were immunoprecipitated with anti-HA antibody (IP: HA) and were identified with anti-LUC antibody (IB:LUC). IgG antibody as a negative control. (d) GmCIPK6 interacts with GmAKT1 domain in yeast cells. Yeast cells were grown on synthetic defined SD-TL medium and SD-TLHA medium. For each experiment, three independent experiments were repeated with similar results.

GmAKT1 interacts with GmCIPK6 in yeasts and plant cells

Previous findings have shown that plant K⁺ channels, such as AKT1 and HAK5, can be regulated by Ser/Thr protein kinase CIPKs (Lara et al., 2020; Lee et al., 2007). These findings prompted us to investigate whether GmAKT1 could be modified by GmCIPKs in soybeans under salt stress. We initially identified and cloned 26 GmCIPK family members (Figure S2a). Subsequently, we verified the interaction specificity of the C-terminal part of GmAKT1 (named GmAKT1-C) with 26 full-length CIPK family members using yeast two-hybrid (Y2H) assay. Only four of them, GmCIPK4, GmCIPK6, GmCIPK14 and GmCIPK23 interacted with GmAKT1-C, respectively (Figure 3a). The relative expressions of four GmCIPK genes were quantified by RT-qPCR in soybean roots and leaves under salt stress. The results showed that GmCIPK6, GmCIPK14 and GmCIPK23 were upregulated, whereas GmCIPK4 was downregulated in soybean roots and leaves in response to salt stress. Additionally, the expression patterns of GmCIPK6 were higher than other GmCIPKs (Figure S2b). Higher β -GAL activity further suggested a strong interaction between GmAKT1c and GmCIPK6 compared to other GmCIPK proteins (Figure S2c). Consequently, we focused on GmCIPK6 as a putative GmAKT1 interactive protein for further investigation. To further test whether GmAKT1 physically interacts with GmCIPK6 in plant cells, we utilized bimolecular fluorescence complementation (BiFC) and co-immunoprecipitation (Co-IP) assays. The BiFC analysis revealed the YFPN-GmAKT1 and YFPC-GmCIPK6 interaction in *Nicotiana benthamiana* leaves and YFP fluorescence signal of interacting proteins was localized at the plasma membranes (PM) (Figure 3b). Moreover, Co-IP assay showed that N-terminally HA-tagged GmAKT1 and C-terminally cLUC-tagged GmCIPK6 were coexpressed in tobacco leaves and immunoprecipitated together (Figure 3c). Together, these results demonstrated that GmAKT1 interacted with GmCIPK6 in plant cells.

Additionally, the C-terminal of AKT1 consists of CNBD (cyclic nucleotide-binding), ANK (ankyrin repeat) and KHA domain. Among these domains, the ANK domain plays a pivotal structural role in the interaction between CIPKs and AKT1, as demonstrated by previous studies (Lee et al., 2007; Thirupathi, 2020). To investigate which domain of soybean GmAKT1 interacts with GmCIPK6, we aligned the C-terminal region of GmAKT1 with the amino acid sequence of Arabidopsis AKT1 and subsequently divided it into the CNBD, ANK and KHA domains. These domains were cloned and inserted into the pGADT7 vector. Following this, we employed Y2H assays to detect interactions between GmCIPK6 and the CNBD, ANK and KHA domains. The result showed that ANK domain of GmAKT1 interacted with GmCIPK6

in yeast (Figure 3d), suggesting that ANK domain provided specificity for the interaction between GmAKT1 and GmCIPK6.

GmCIPK6 phosphorylates GmAKT1

Considering that GmCIPK6 interacts with GmAKT1 and functions as a protein kinase, we investigated whether GmAKT1 undergoes phosphorylation using a phosphate affinity Mn²⁺-Phos-tag SDS-PAGE assay. When Phos-tag specifically combined to phosphate ions, it decreases the electrophoretic mobility of phosphorylated proteins compared to non-phosphorylated proteins (Mao et al., 2011). In our assays, standard SDS-PAGE generated a single GmAKT1-HA protein band (Figure 4a), whereas Mn²⁺-Phos-tag SDS-PAGE showed different mobility in GmAKT1-HA bands (Figure 4b). Furthermore, treatment of GmAKT1-HA protein extracts with calf intestinal phosphatase (CIP) accelerated the mobility shift observed in the Mn²⁺-Phos-tag SDS-PAGE, implying a reduction in the phosphorylation level of GmAKT1 (Figure 4b). These results confirmed that GmAKT1 could be phosphorylated by kinases in soybean.

To further determine whether GmAKT1 could be phosphorylated by GmCIPK6, GmAKT1c-MBP (C-terminal intracellular domain of GmAKT1) and GmCIPK6-His proteins were firstly obtained from the BL21 *Escherichia coli*. Then, we separated GmAKT1c-MBP and GmCIPK6-His proteins using an Mn²⁺-Phos-tag gel and detected them by immunoblot analysis. The results showed that the phosphorylation bands of GmAKT1-MBP were detected by adding GmCIPK6-His protein, indicating that GmAKT1 could be phosphorylated by GmCIPK6 (Figure 4c). Additionally, due to AKT1 could be phosphorylated by CIPKs, we inferred that phosphorylation sites of GmAKT1 were conserved in plants. Previous research has shown that SOS2/CIPK24 phosphorylates hydrophobic-X-basic-X(2)-S/TX(3)-hydrophobic motifs (Gong et al., 2002). Therefore, we aligned the amino acid sequences of GmAKT1 and AKT1 and found that residue S730 of GmAKT1 might be a potential phosphorylation site (Figure S3). To confirm specific phosphorylation site, we mutated S730 of GmAKT1 residues to alanine (A) individually to mimic non-phosphorylated state (S730A). This mutation resulted in the abolition of GmAKT1-MBP S730A phosphorylation, and the bands were weakened (Figure 4c), indicating that S730 of GmAKT1 is a key site for GmCIPK6 to phosphorylate GmAKT1.

GmCBL9 is involved in upstream regulation of GmCIPK6

Studies showed that the activity of CIPKs is modulated by CBLs in plants (Luan et al., 2002). To verify whether Ca²⁺ sensor GmCBLs interact with GmCIPK6, we initially identified and cloned 10 GmCBL genes in soybean (Figure S4a). Furthermore, Y2H assay was applied to screen for interaction between

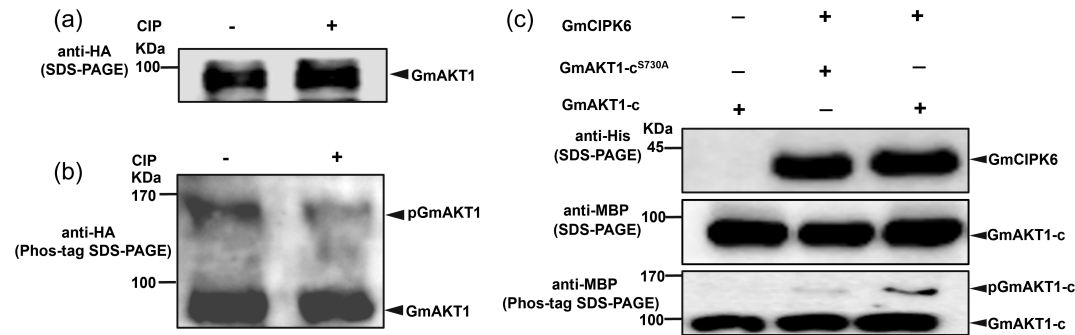


Figure 4 GmAKT1 is phosphorylated by GmCIPK6. (a, b) Western blot showing the phosphorylation of GmAKT1 in soybean with Mn^{2+} -Phos-tag SDS-PAGE. SDS-PAGE as control for GmAKT1-HA expression. Protein extracts were treated with or without calf intestinal phosphatase (CIP) and immunoblot detected with anti-HA antibody. (c) Purified recombinant protein GmAKT1-c-MBP, GmAKT1-c^{S730A}-MBP and GmCIPK6-His were incubated together and detected by western blot with SDS-PAGE and Mn^{2+} -Phos-tag SDS-PAGE. All experiments included three biological replicates.

GmCIPK6 with GmCBLs. The results showed that GmCBL1, GmCBL2, GmCBL9 and GmCBL10 could interact with GmCIPK6 (Figure 5a). We further analysed the relative expression of four *GmCBL* genes (*GmCBL1*, *GmCBL2*, *GmCBL9* and *GmCBL10*) in soybean. Under salt stress, *GmCBL9* was obviously upregulated compared to other *GmCBL* genes in soybean roots and leaves (Figure S4b). Additionally, the β -GAL activity analysis confirmed the strong interaction between GmCBL9 and GmCIPK6 (Figure S4c). Thus, we selected GmCBL9 as a candidate for the GmCBL-GmCIPK complex mechanism in soybean. *In vivo* BiFC and Co-IP assays confirmed the interaction between GmCBL9 and GmCIPK6. We detected the YFP fluorescent signals of GmCBL9-GmCIPK6 interaction in the plasma membrane (PM) of *Nicotiana benthamiana* cells (Figure 5b). Co-IP assay proved that GmCBL9-FLAG with GmCIPK6-cLUC was successfully co-immunoprecipitated (Figure 5c). Taken together, these results indicated that GmCBL9 interacted with GmCIPK6 *in vitro* and *in vivo*.

Notably, we also found that both GmAKT1-GmCIPK6 and GmCBL9-GmCIPK6 were localized at the plasma membrane (PM) based on BiFC assays (Figures 3b and 5b). Interestingly, subcellular localization analysis of the three proteins (GmCBL9, GmCIPK6 and GmAKT1) revealed that GmAKT1 and GmCBL9 were localized to the PM, while GmCIPK6 was localized in the nucleus (Figure S5). Combining these results with previous studies (Li *et al.*, 2014), we suggested that GmCBL9 might recruit GmCIPK6 to the PM, where GmCIPK6 could interact with PM-located GmAKT1.

GmCBL9-GmCIPK6-dependent activation of GmAKT1 in yeasts and HEK293 cells

To reveal whether GmAKT1 could be regulated by GmCBL9-GmCIPK6 complex, we individually expressed various combinations of these proteins (*GmCBL9*, *GmCIPK6*, *GmAKT1*, *GmCBL9-GmCIPK6*, *GmCBL9-GmAKT1*, *GmCIPK6-GmAKT1* and *GmCBL9-GmCIPK6-GmAKT1*) in K^+ -uptake-deficient yeast mutant (R5421) system. The objective was to assess their impact on growth in AP medium supplemented with different concentrations of K^+ or NaCl. Our results showed that all groups could grow on AP medium under normal conditions (50 mM K^+) (Figure 6d). However, yeast mutants expressing *GmCBL9*, *GmCIPK6* or *GmCBL9-GmCIPK6* could not grow on AP medium containing low K^+ concentrations (0.05, 0.5 and 1 mM K^+)

(Figure 6a–c). Remarkably, the coexpression of *GmCBL9*, *GmCIPK6* and *GmAKT1* genes significantly improved yeast growth under low K^+ conditions (Figure 6a–c). These results showed that GmAKT1 mediated K^+ uptake by GmCBL9-GmCIPK6 complex (Figure 6a–c). Additionally, we discovered that coexpression of *GmCBL9*, *GmCIPK6* and *GmAKT1* improved salt tolerance in yeast under 400 mM NaCl stress (Figure 6e). The result confirmed that the GmCBL9-GmCIPK6 complex could regulate GmAKT1-mediated K^+ absorption to enhance salt tolerance.

Considering that the activation of transporters and channels mediated by the CBLs-CIPKs complex depends on Ca^{2+} in plants (Li *et al.*, 2014; Nieves-Cordones *et al.*, 2023), we investigated whether the GmCBL9-GmCIPK6 complex regulates GmAKT1-mediated K^+ absorption in a Ca^{2+} -dependent manner. Therefore, we mutated the fourth EF-hand of GmCBL9, which is responsible for Ca^{2+} binding, namely *GmCBL9*^{E172Q}. Subsequently, *GmAKT1*, *GmCBL9-GmCIPK6-GmAKT1* and *GmCBL9*^{E172Q}-*GmCIPK6-GmAKT1* were transfected and coexpressed in HEK293T cells, respectively. The results showed that the mutation of *GmCBL9* decreased GmAKT1-mediated K^+ absorption (Figure 7d, e), confirming that the activity of GmAKT1 is dependent on Ca^{2+} signal. Furthermore, we identified that the coexpression of *GmCBL9-GmCIPK6-GmAKT1* significantly increased inward rectifying K^+ currents compared with transfecting *GmAKT1* alone in HEK293T cells (Figure 7a, b, e), which indicated that GmCBL9-GmCIPK6 complex could enhance GmAKT1-mediated inward rectifying K^+ currents. Additionally, we found that the inward rectifying K^+ currents in HEK293T cells expressing *GmCBL9-GmCIPK6-GmAKT1*^{S730A} (the mutation of GmAKT1 phosphorylation site) were lower than those in cells coexpressing *GmCBL9-GmCIPK6-GmAKT1* in HEK293 cells (Figure 7c, e). Taken together, these results provide evidence that the activity of GmAKT1 depends on the phosphorylation regulation by the Ca^{2+} -GmCBL9-GmCIPK6 complex.

GmCBL9-GmCIPK6-GmAKT1 module improved salt tolerance in soybean

To further investigate whether GmCBL9-GmCIPK6 complex could positively regulate GmAKT1-mediated K^+ uptake in soybean under salt stress, we first transformed *GmCBL9* and *GmCIPK6* in yeasts (INVSc1) and transgenic soybean hairy roots, respectively.

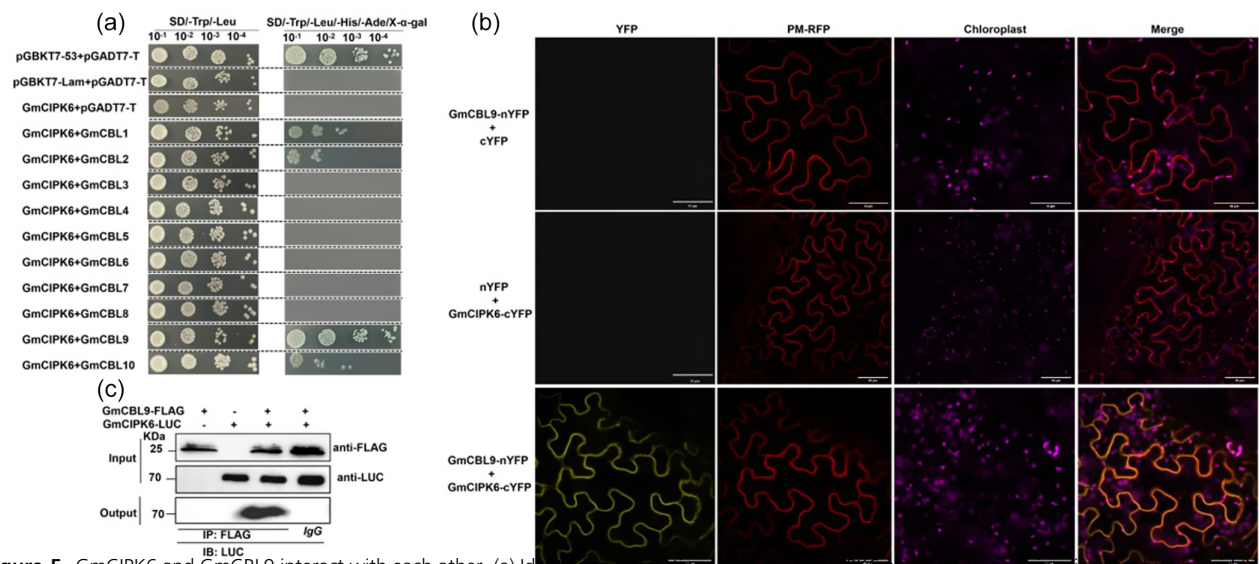


Figure 5 GmCIPK6 and GmCBL9 interact with each other. (a) Identifying interactions between GmCIPK6 and GmCBL proteins via yeast two hybrid (Y2H) assay. Transformed yeast cells were grown on SD medium (lacking Leu and Trp) or (lacking Leu, Trp, His and Ade). The combination pGBKT7-53 and pGADT7-T was used as a positive control, and pGBKT7-lam + pGADT7-T and GmCIPK6+ pGADT7-T were used as a negative control. (b) Bimolecular fluorescence complementation (BiFC) reveals the interaction between GmCIPK6 and GmCBL9 in tobacco leaves. The N- and C-terminal fragments of YFP were linked to the GmCBL9 and GmCIPK6, respectively. GmCBL9-nYFP+cYFP and nYFP+GmCIPK6-cYFP were used as negative control. PM-RFP as a cell membrane marker. Scale bars are 50 μ M. (c) Co-IP assay showing the interaction between GmCIPK6 and GmCBL9. GmCBL9-FLAG and GmCIPK6-LUC were expressed in tobacco and then used for Co-IP assays. Anti-FLAG and anti-LUC antibodies were used to detect GmCBL9-FLAG and GmCIPK6-LUC, respectively. Three independent experiments were performed in this study.

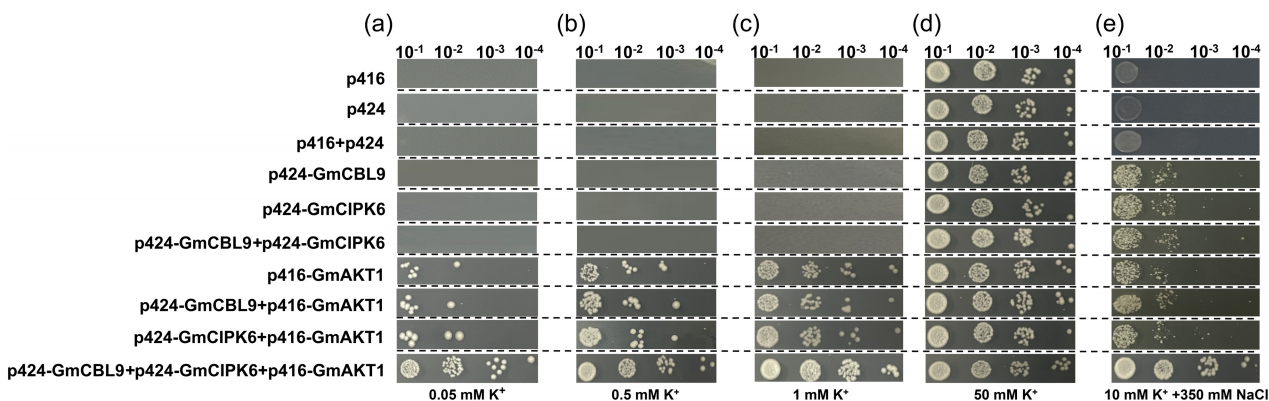


Figure 6 Coexpression of GmCBL9 and GmCIPK6 enhances GmAKT1 mediated K^+ -uptake activity. (a–c) GmCBL9-GmCIPK6 improves the growth of K^+ -uptake-deficient yeast mutant R5421 expressing *GmAKT1* on different K^+ AP medium. (d) The GmAKT1-mediated regulation of K^+ involving GmCBL9 and GmCIPK6 enhances yeast growth on a salt medium. *GmAKT1*, *GmCBL9* and *GmCIPK6* were constructed into p416 and p424 vectors, respectively. The 1:10 serial dilutions (as a black triangle) of yeast cells were spotted on the AP medium.

After salt treatment, yeast overexpressing *GmCBL9* or *GmCIPK6* exhibited improved salt tolerance compared to yeast containing the pYES2 vector alone (Figure S6a). Similarly, overexpression of *GmCBL9* and *GmCIPK6* in transgenic soybean hairy roots enhanced salt tolerance by increasing K^+ and decreasing Na^+ content (Figure S6b–h). These results demonstrate that *GmCBL9* and *GmCIPK6* could positively regulate salt tolerance in soybean. Furthermore, we coexpressed *GmCBL9* and *GmCIPK6* genes in WT, *GmAKT1-OE* and *GmAKT1-KO* backgrounds, generating composite transgenic soybean hairy roots. During the salt stress, composite transgenic soybean hairy roots in the *GmAKT1-OE* background showed larger roots and greener leaves compared to those in the WT and *GmAKT1-KO* backgrounds (Figure 8a).

Moreover, the composite transgenic soybean hairy roots in the *GmAKT1-OE* background had significantly higher K^+ content and lower Na^+ content than those in the WT and *GmAKT1-KO* plants under salt stress (Figure 8b–d). Thus, these results demonstrated that the GmCBL9-GmCIPK6 complex promoted GmAKT1-mediated K^+ uptake, thereby balancing the Na^+/K^+ ratio and improving salt tolerance in soybeans (Figure 9).

Discussion

Soybean (*Glycine max* (L.) Merr.) is an important legume crop that provides plentiful vegetable oil and protein (Graham and Vance, 2003). However, salt stress has harmful effects on

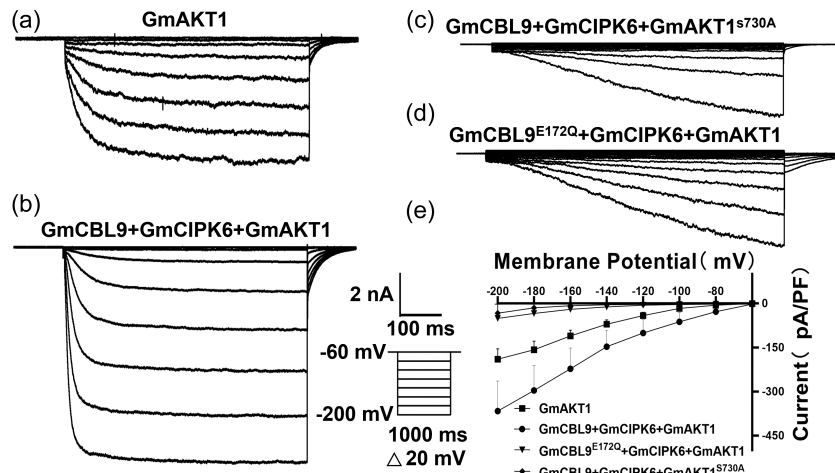


Figure 7 GmAKT1-mediated K⁺ inward currents are activated by GmCBL9 and GmCIPK6 in HEK293 cells. (a–d) Patch-clamp whole-cell recordings of inward K⁺ currents in HEK293 cells expressing different combinations of GmAKT1, GmCBL9-GmCIPK6-GmAKT1, GmCBL9-GmCIPK6-GmAKT1^{S730A} and GmCBL9^{E172Q}-GmCIPK6-GmAKT1. The voltage protocols, as well as time and current scale bars for the recordings, are shown. (e) The I-V relationship of the steady state whole-cell inward K⁺ currents in HEK293 cells. The data are derived from the recordings as shown in (a–d) and presented as means ± SE.

soybean growth and development, resulting in lower yield and quality (Phang *et al.*, 2008). Therefore, it is critical to identify and exploit salt-tolerant genes to breed soybean cultivars with enhanced salt tolerance. In this study, we investigated the salt tolerance of K⁺ channel gene *GmAKT1* in soybean and characterized a GmCBL9-GmCIPK6 complex that regulates GmAKT1-mediated K⁺ uptake, thereby conferring salt tolerance of soybean.

During salt stress, excessive Na⁺ interferes with K⁺ uptake in plants, leading to cellular damage and nutrient deficiency (Li *et al.*, 2023). Therefore, maintaining cellular Na⁺/K⁺ balance is a critical feature of plant survival under salt stress (Yang and Guo, 2018). Previous studies have demonstrated that some ion channels or transporters can regulate plants Na⁺/K⁺ balance by increasing K⁺ influx or Na⁺ efflux in response to salt stress (Zhu, 2016; Van Zelm *et al.*, 2020; Wang *et al.*, 2020). However, the salt tolerance of the K⁺ channels or transporters is largely unknown compared to Na⁺ transporters in soybean under salt stress (Jia *et al.*, 2021; Sun *et al.*, 2019; Zhang *et al.*, 2021). In this study, we identified a soybean K⁺ channel gene *GmAKT1*, which mediates K⁺ absorption by the validation of heterologous expression systems (Figures 1a–c and 7a). Notably, AKT1 is a major system of K⁺-uptake, which could mediate K⁺ influx and improve the salt tolerance of plants (Li *et al.*, 2019, 2023; Ma *et al.*, 2017). Furthermore, we characterized the function of the K⁺ channel gene *GmAKT1* in transgenic soybeans (*GmAKT1*-OE and *GmAKT1*-KO lines) under salt stress. Phenotypic analysis revealed that the leaves of *GmAKT1*-OE lines were greener than *GmAKT1*-KO lines under salt stress (Figure 2a). Additional physiological results indicated that *GmAKT1*-OE lines had significantly higher K⁺ and lower Na⁺ content compared to *GmAKT1*-KO lines under salt stress (Figure 2f–k). Thus, these findings proved that GmAKT1-mediated K⁺ influx could maintain Na⁺/K⁺ balance, thereby enhancing salt tolerance in soybean.

Some studies have shown that AKT1-mediated influx K⁺ currents could be regulated by different CBL-CIPK complexes in plants (Han *et al.*, 2021; Lee *et al.*, 2007; Xu *et al.*, 2006). However, the current study regarding soybean GmAKT1 involved in the regulation of GmCBL-GmCIPK complexes remains

unknown. In this study, we identified that GmCBL9 interacted with GmCIPK6 and GmCIPK6 interacted with GmAKT1 in soybean (Figures 3a–c and 5a–c). Furthermore, we observed that the coexpression of *GmCBL9*, *GmCIPK6* and *GmAKT1* in yeast and HEK293T cells enhanced K⁺ influx currents (Figures 6a–c and 7b). These findings indicated that the GmCBL9-GmCIPK6 complex was necessary for modulating GmAKT1-mediated K⁺ uptake in soybean. Remarkably, the CBL-CIPK complexes, as a critical signalling transducer for plants, regulate the activity of ion channels and transporters in response to salt stress. For instance, the SOS1 transporter can be activated by the CBL4/CBL8-CIPK24 complex, facilitating Na⁺ efflux and improving salt tolerance of Arabidopsis (Qiu *et al.*, 2002; Quintero *et al.*, 2011). Similarly, the voltage-gated K⁺ channel HbVGKC1 could be activated by HbCBL1-HbCIPK2 complex under salt stress in wild barley (Zhang *et al.*, 2020). Interestingly, we found that overexpression of *GmCBL9* or *GmCIPK6* in soybeans increased K⁺ influx, thereby reducing Na⁺ content under salt stress (Figure S5b–h). Additionally, composite transgenic soybean hairy roots in the *GmAKT1*-OE background had significantly higher K⁺ and lower Na⁺ concentrations compared with WT or *GmAKT1*-KO plants in response to salt stress (Figure 8b, c). These results suggested that GmCBL9-GmCIPK6 complex positively regulated GmAKT1-mediated K⁺ uptake in soybeans under salt stress.

It is noteworthy that the critical roles of CBL-CIPK complexes depend on Ca²⁺, which facilitates the formation of regulatory complexes and enhances the kinase activity, thus activating ion channels and transporters in the adaptation of plants to adverse environmental stresses (Mao *et al.*, 2023; Tang *et al.*, 2020). However, it was unknown how the GmCBL9-GmCIPK6 complex triggers the GmAKT1-mediated K⁺ absorption in soybean. Studies have demonstrated that salt stress initiates primary calcium signals, which are primarily sensed by calcium sensors, such as CBLs. These sensors can activate downstream signalling networks that regulate plant physiological processes (Dong *et al.*, 2022; Kiegle *et al.*, 2000; Steinhorst *et al.*, 2022). In plants, CBLs contain EF-hand domains that perform the basic and common function of binding Ca²⁺ (Luan *et al.*, 2002; Mohanta *et al.*, 2019). In this study, we demonstrated that coexpression of

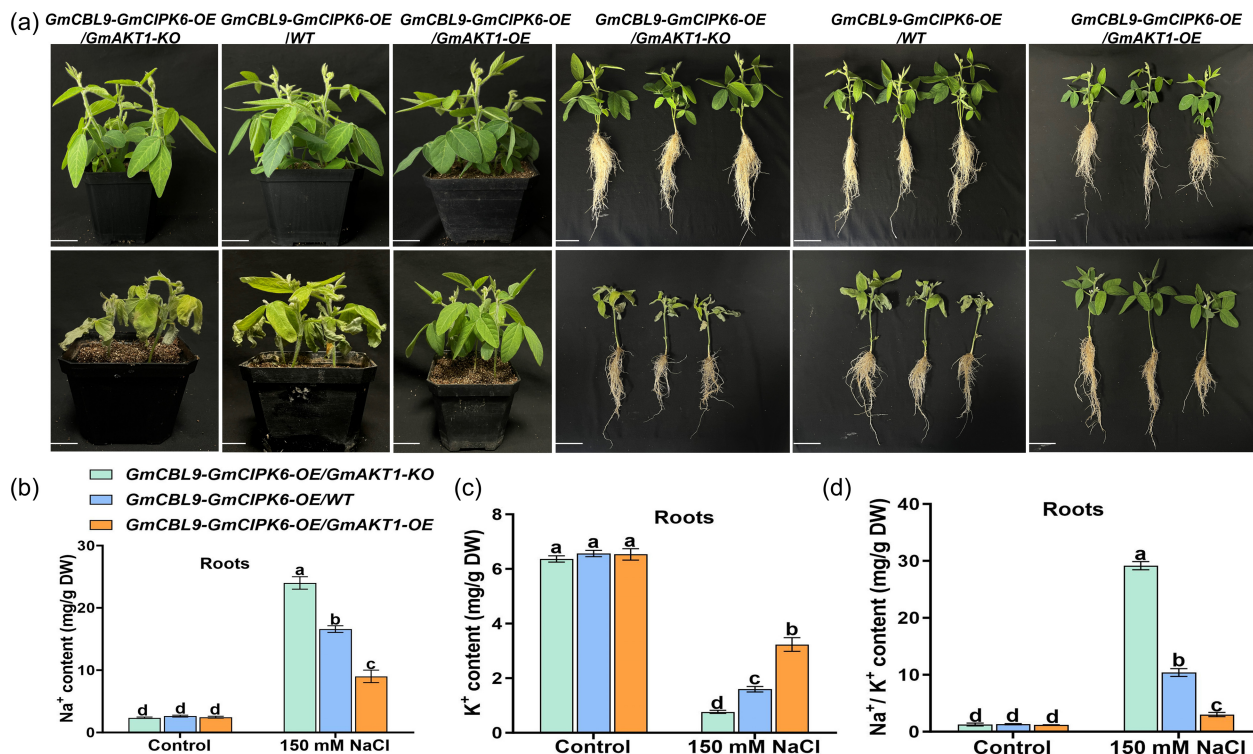


Figure 8 Soybean K⁺ channel GmAKT1 enhances salt-tolerant capacity by the regulation of GmCBL9-GmCIPK6 complex. (a) Soybean plant phenotypes under normal and salt stress conditions. Bars, 2 cm. *GmCBL9-GmCIPK6-OE/GmAKT1-KO* hairy roots in the *GmAKT1-KO* background, *GmCBL9-GmCIPK6-OE/WT* hairy roots in the WT (DN50) background, and *GmCBL9-GmCIPK6-OE/GmAKT1-OE* hairy roots in the *GmAKT1-OE* background. Data are the mean \pm SD of $n = 3$. (b and d) Na⁺ content, K⁺ content and Na⁺/K⁺ ratio of *GmCBL9-GmCIPK6-OE/GmAKT1-KO*, *GmCBL9-GmCIPK6-OE/WT* and *GmCBL9-GmCIPK6-OE/GmAKT1-OE* hairy roots under normal and 150 mM salt stress. $n \geq 30$ plants per genotype. Different letters indicate statistically significant differences at $P < 0.05$ by two-way ANOVA and Student's t -test.

GmCBL9^{E172Q} (the mutation of the fourth GmCBL9 EF-hand), *GmCIPK6* and *GmAKT1* into HEK293T cells resulted in lower K⁺ influx currents compared to coexpression of *GmCBL9*, *GmCIPK6* and *GmAKT1* in HEK293T cells (Figure 7d, e), and this result was also similar with previous reports in rice (Li et al., 2014). Our findings indicated that GmCBL9 played a role in accepting Ca²⁺ and the regulation of GmCBL9-GmCIPK6-GmAKT1 module. Additionally, CBL1/9 can bind to CIPK23 to form CBL1/9-CIPK23 complex, which decodes Ca²⁺ signal, thus phosphorylates AKT1 and promotes K⁺ influx currents in Arabidopsis (Xu et al., 2006). Furthermore, CBL1/9-activated CIPK1 directly phosphorylates ABA receptor PYLs, negatively modulating drought response (You et al., 2023). These studies show that downstream proteins are phosphorylated by Ca²⁺-CBLs-activated CIPKs in plants. We also demonstrated that GmAKT1 is involved in the regulation of phosphorylation in soybeans (Figure 4b). Mn²⁺-Phos-tag mobility assays revealed that GmAKT1 could be phosphorylated by GmCIPK6 and the 735S site of GmAKT1 is necessary for the phosphorylation regulation by GmCIPK6 (Figure 4c). Remarkably, GmAKT1^{S730A} (the mutation phosphorylation site of GmAKT1) also lowered K⁺ influx currents in HEK293T cells (Figure 7c, e). Consequently, these data suggested that GmCIPK6 mediated phosphorylation of GmAKT1 triggers the K⁺ uptake. Interestingly, our findings also showed that both GmCBL9 and GmAKT1 were located on PM, and GmCIPK6 were located on nucleus in tobacco epidermal cells (Figure S4), whereas coexpression of GmCBL9 and GmCIPK6 or coexpression of GmAKT1 and GmCIPK6 were located on PM

(Figures 3b and 5b). Taken together, these findings suggested that GmCBL9 might recruit GmCIPK6 to PM, resulting in GmCIPK6 interacting with and phosphorylating plasma membrane-located GmAKT1.

In summary, we propose a regulatory model for GmCBL9-GmCIPK6-GmAKT1-mediated K⁺ in soybean. Salt stress triggered GmCBL9 interacted with and activated GmCIPK6 to phosphorylate GmAKT1 to mediate K⁺ uptake, thus maintaining Na⁺/K⁺ balance and enhancing salt tolerance of soybean (Figure 9). These findings may expand our comprehension of salt stress responses and provide potential genetic resources for generating salt-tolerant soybean varieties.

Methods

Plant materials, growth conditions and simulated salt stress treatment

For the identification of gene expression pattern, the soybean ('Dongnong 50') seedlings at fully expanded first trifoliate leaf stage were treated with 1/2 strength Hoagland nutrient solution containing NaCl (120 mM). The soybean leaves and roots were harvested at different time intervals (0 h, 1 h, 3 h, 6 h and 12 h).

For the phenotype of stable-transgenic soybean plants, the soybean seeds were grown in glasshouse (16 h light/8 h dark, 25 °C, 60% relative humidity) using soil and vermiculite (1:1 ratio). The soybean plants were immersed in 150 mM NaCl with 1/2 strength Hoagland nutrient solution each day when the first

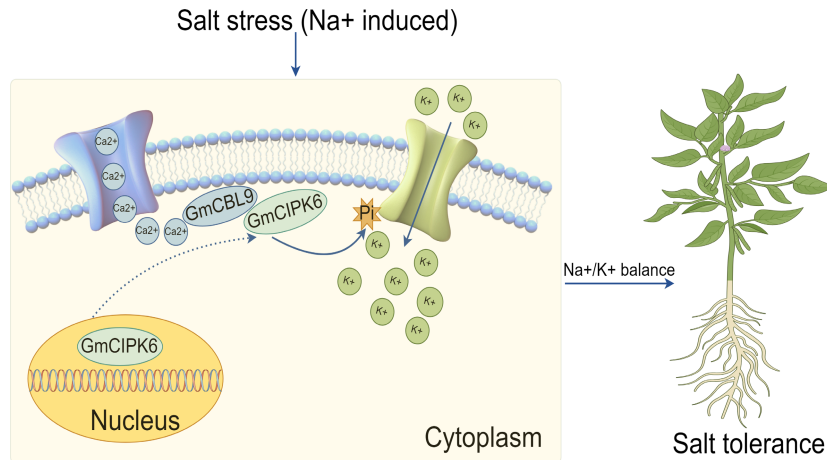


Figure 9 A proposed model for GmCBL9-GmCIPK6-GmAKT1 module mediated salt stress response in soybean. Under salt stress, Ca^{2+} sensor GmCBL9 interacts with protein kinase GmCIPK6 and recruits GmCIPK6 to the plasma membrane where they phosphorylate and activate GmAKT1-mediated K^{+} uptake, thus keeping $\text{Na}^{+}/\text{K}^{+}$ ratio and enhancing salt tolerance of soybean.

trifoliate leaves were fully expanded. Twenty-three days after salt treatment, growth parameters were measured.

For Arabidopsis assays, the seeds were germinated on 1/2 MS (Murashige and Skoog) medium containing 8% agar and 20% sucrose in a growth chamber (14 h light/ 10 h dark, 23 °C, 60% relative humidity). For phenotypic analysis, 7-day-old seedlings were transferred to 1/2 MS medium with different K^{+} concentrations for 16 days.

Vector construction and soybean transformation

To construct overexpression vector *GmAKT1*, the CDS (coding sequence) of *GmAKT1* containing HA-tag was cloned into the pCAMBIA3301 vector using Seamless Cloning (Vazyme, C112). In order to knock down *GmAKT1*, the sgRNAs (single-guide RNAs) targeting *GmAKT1* were designed using online tool CRISPR-P (<http://crispr.hzau.edu.cn/cgi-bin/CRISPR2/CRISPR>), and subsequently synthesized and ligated into the pGES-201 vector. All primer sequences used are listed in Table S1.

To generate stable-transgenic soybean plants, recombinant plasmids were transferred into *Agrobacterium* strain EHA105, respectively. Subsequently, soybean 'DN50' served as the recipient material for the transformation following the method described previously by Zhao *et al.* (2018). *GmAKT1*-overexpressing soybean lines were identified by RT-qPCR. The loss-of-function mutants were screened by DNA sequencing. Primers are listed in Table S1.

RNA extraction and RT-qPCR analysis

To analyse the expression pattern of genes, total RNA was extracted from plant tissues using RNAiso Plus according to the manufacturer's protocol (Takara). The cDNA was synthesized using the PrimeScriptTM RT reagent Kit (Takara) and served as a template for RT-qPCR, which was performed using the SYBR Premix ExTaq kit (Takara) on the AriaMx real-time PCR system (Agilent). The primer sequences used for RT-PCR and other experiments are listed in Supplemental Table S1.

Ion concentration analysis

For kinetic analysis of *GmAKT1* K^{+} uptake in Arabidopsis, 12-d-old seedlings (WT, *atakt1* and *atakt1-GmAKT1*) were treated in

starvation solution (0.2 mM CaSO_4 and 5 mM MES, pH 5.7) at 28 °C for 48 h. A 0.8 g fresh seedlings were transferred into depletion solution (0.25 mM KNO_3 , 0.2 mM CaSO_4 and 5 mM MES, pH 5.7). The solution samples were collected at various time points as indicated, and K^{+} content was measured by flame spectrophotometer (Sherwood, M410).

For Na^{+} and K^{+} content measurements in soybean roots and leaves, the samples were collected after 23 days of salt treatment. The plant tissues were dried in an oven at 105 °C for 30 min, followed by drying at 80 °C for 3 days. The dry samples were then extracted with sulfuric acid for 8 h and subsequently dissolved using 30% hydrogen peroxide. Finally, the Na^{+} and K^{+} contents were determined using a flame spectrophotometer (Sherwood M410).

Yeast complementation assays

The CDS of *GmAKT1* was constructed and ligated into the p416-GPD vector, while *GmCBL9* and *GmCIPK6* were constructed and ligated into the p424-GPD vector. Subsequently, these recombinant plasmids were transformed into the K^{+} -deficient yeast strain R5421 (*trk1Δ trk2Δ*). Single yeast cell was selected and cultured in SD medium including 100 mM KCl until the optical density at OD₆₀₀ reached 1.0. The transformations of cells were collected by centrifugation and washed three times. The yeast cells were suspended in deionized water to OD₆₀₀ of 0.8. Finally, the cells were diluted 10-fold and incubated on arginine phosphate (AP) medium containing different concentrations of K^{+} or 350 mM Na^{+} with 10 mM K^{+} for 4 days. Primer sequences are listed in Table S1.

Y2H assays

The cytosolic region of GmAKT1-C, along with 10 genes from the *GmCBL* family, were cloned into the pGBKT7 vector, while the coding sequences of 26 genes from the *GmCIPK* family were fused into the pGADT7 vector. The group of pGBKT7-53 and pGADT7-T were used as positive control, pGBKT7-lam and pGADT7-T were used as negative control. The respective AD and BD plasmids were co-transformed into AH109 yeast strain and tested for growth in selective medium SD-TL (tryptophane and leucine) and SD-TLH (tryptophane, leucine

and histidine) at 30 °C. After 5 days, β -galactosidase activity was detected using the ONPG assay (Coolaber, YK3030) and the plates were photographed. Primer sequences are listed in Table S1.

BiFC assays

The CDS of *GmAKT1* and *GmCBL9* were fused and cloned into pXY104 vector including the N-terminal of YFP, and *GmCIPK6* was constructed into pXY106 vector containing the C-terminal of YFP. Both of these plasmids were transformed into *Agrobacterium tumefaciens* strain GV3101 (pSoup-p19), and the BiFC assay was performed as described previously (Waadt et al., 2008). Fluorescence signal of YFP (excited at 488 nm and emitted between 520 and 560 nm) in the transformed leaves of *Nicotiana benthamiana* was detected using a laser scanning confocal microscope (Zeiss, LSM980). Primer sequences are listed in Table S1.

Co-IP assays

GmAKT1-HA (*GmAKT1* fused with 3 \times HA-tag) and *GmCBL9*-FLAG (*GmCBL9* fused with 3 \times FLAG) were constructed into pCambia1300-NLuc, and the CDS of *GmCIPK6* was constructed into pCambia1300-CLuc. The fusion constructs were transformed into *Agrobacterium tumefaciens* strain GV3101 (pSoup-p19), respectively. The tested construct pairings were expressed in *Nicotiana benthamiana* leaves for 2 days, and these assays were applied using the Co-IP kit (BersinBio, Bes3011). Briefly, the total proteins were extracted using a cell lysis buffer containing protease inhibitors. Then, the proteins were immunoprecipitated by anti-HA (Sigma, GT423) or anti-FLAG antibody (Sigma, F1804) according to the group of experiments, and later the products were incubated via Protein A/G-MagBeads. Finally, the precipitates were detected using anti-CLUC antibody (Sigma, L2164) and anti-IgG (as negative control). Primer sequences are listed in Table S1.

Subcellular localization

The CDS of *GmAKT1*, *GmCBL9* and *GmCIPK6* without stop codon were amplified and constructed into pMDC43::GFP expression vector. The recombinant plasmids were transformed into *Arabidopsis* protoplast, as Jin et al. (2001) described. The pMDC43::GFP vector was used as the negative control. After 16 h, the transformed protoplasts were imaged using a confocal microscope (Zeiss, LSM980). Primer sequences are listed in Table S1.

Expression and purification of recombinant proteins

The cytosolic region of *GmAKT1*-C was constructed into pMAL-C2X expression vector to generate MBP-*GmAKT1*, and the CDS of *GmCIPK6* was cloned into pHis-28a vector to generate *GmCIPK6*-His. The recombinant expression vectors were transformed into *Escherichia coli* strain BL21 and were induced with 0.5 mM β -D-thiogalactopyranoside (IPTG) at 16 °C for 12 h. Subsequently, the MBP-*GmAKT1* fusion proteins were purified by MBP-Tag protein purification kit (Abbkine, KTP2020) and the *GmCIPK6*-His proteins were purified using His-Tag protein purification kit (Beyotime, P2226). Primers are listed in Table S1.

The analysis of protein phosphorylation in vivo and in vitro

For the phosphorylation detection of *GmAKT1* in vivo, soybean leaves expressing *GmAKT1* with an HA-tag were extracted using protein lysis buffer (50 mM HEPES pH 7.5, 150 mM KCl, 1 mM

EDTA, 0.5% TritonX-100, 1 mM DTT, 1 \times protease inhibitors), and then the protein concentration were determined according to the manufacturer's instructions for the bicinchoninic acid (BCA) protein assay kit (Solarbio, PC0020). The protein, treated with or without CIP (Sigma, P0114), were incubated for 12 h at 37 °C. The products were separated on 10% Mn^{2+} -Phos-tag SDS-PAGE gels (Wako, 304-93521) and 10% SDS-PAGE gels (as a control), and the assay of electrophoresis and western blot performed as reported previously (Bekešová et al., 2015). The proteins were immunoblotted with anti-HA antibody (Sigma, H9658).

For the detection of protein phosphorylation in vitro, the MBP-tagged purified *GmAKT1*-C (2 μ g per reaction) and the different concentrations of kinase protein *GmCIPK6*-His (0.2 μ g or 0.4 μ g per reaction) were mixed in 50 μ L reaction solution, respectively (20 mM Tris-HCl, pH 7.5, 2.5 mM $MnCl_2$, 2.5 mM $MgCl_2$, 0.5 mM $CaCl_2$, 1 mM DTT, 0.2 mM ATP), respectively. After incubation at 30 °C for 30 min, protein phosphorylation was determined according to the above description. The proteins were immunoblotted using an anti-MBP antibody (Trans, HT701-01).

Patch-clamp recording from HEK293T cells

For electrophysiological characterization of *GmAKT1* in HEK293T cells, *GmAKT1*, *GmAKT1*^{S730A}, *GmCBL9*, *GmCBL9*^{E172Q} and *GmCIPK6* were amplified and ligated into pB513B-1 vector, respectively. HEK293T cells were cultured as described previously (Gao et al., 2016). Then, the recombinant plasmids were transfected into HEK293T cells using lipofectamine 3000 transfection reagent (Thermo, L3000001). After 24 h, the transfected cells were suspended using Trypsin-EDTA solution (Solarbio, T1320) and were centrifuged at 1000 rpm for 5 min. For recordings of *GmAKT1*-mediated K^+ currents, the cells exhibiting GFP fluorescence were selected and the cells were measured with a patch-clamp setup comprising an AxoClamp 900A Amplifier. Whole-cell current recordings were performed via voltage step protocol ranging from -200 to -60 mV at a holding potential of -80 mV. The pipette solution and bath solution were prepared according to previous descriptions (Fuchs et al., 2005; Li et al., 2014). Primer sequences are listed in Table S1.

The induction of soybean hairy roots and phenotypic analysis under salt stress

To create composite plants of soybeans, the transgenic soybean hairy roots were generated as described by Kereszt et al. (2007) with some modifications. Briefly, soybean seeds were germinated in vermiculite and then *Agrobacterium rhizogenes* harbouring *GmCBL9*, *GmCIPK6* and *GmCBL9*-*GmCIPK6* were injected into the hypocotyls of 5-day-old soybean seedlings. After growing in humidity for 6 days, the wound sites were covered with vermiculite for 15 days until hairy roots were approximately 10 cm long. The seedlings were treated with or without 150 mM NaCl for 10 days. The content of Na^+ and K^+ was measured by flame spectrophotometer (Sherwood, M410). All experiments were performed with a minimum of three biological repetitions.

Statistical analyses

All experiments were repeated at least three times. For the comparison between two samples, the data were analysed

according to the Student's *t*-test. For multiple comparisons, the data were carried out by one-way analysis of variance (ANOVA).

Acknowledgements

We thank Professor Yi Wang (China Agricultural University) for providing Arabidopsis mutant *atakt1* and yeast strains R5421 and Professor Wenhua Zhang (Nanjing Agricultural University) for providing the vectors p416-GPD and p424-GPD vectors.

Funding

This work was supported by the Biological Breeding-National Science and Technology Major Project (2023ZD04073), the National Natural Science Foundation of China (32171937, 32201716, 32301751 and 32301921) and the China Postdoctoral Science Foundation (2024M750700).

Conflict of interest

The authors declare no competing interests.

Author contributions

F. C. designed and interpreted the results. L.H.Y. and Z.Y.G. supervised the experiments the projects. F.C., M.A.H., Z.Y., W.Y.N., S.Y.Y., L.Y.X., G.H.T., J.Y., X.K.H. and Z.W.P. performed the experiments. F.C. performed the data analysis. F.C. wrote the manuscript. L.H.Y. and M.A.H. revised the manuscript. All authors read and approved the final manuscript.

Data availability statement

The data that supports the findings of this study are available in the supplementary material of this article.

References

Alvarez-Aragon, R., Haro, R., Benito, B. and Rodriguez-Navarro, A. (2016) Salt intolerance in Arabidopsis: shoot and root sodium toxicity, and inhibition by sodium-plus-potassium overaccumulation. *Planta* **243**, 97–114.

Ardie, S.W., Liu, S. and Takano, T. (2010) Expression of the AKT1-type K(+) channel gene from *Puccinellia tenuiflora*, PutAKT1, enhances salt tolerance in Arabidopsis. *Plant Cell Rep.* **29**, 865–874.

Bailey-Serres, J., Parker, J.E., Ainsworth, E.A., Oldroyd, G.E.D. and Schroeder, J.I. (2019) Genetic strategies for improving crop yields. *Nature* **575**, 109–118.

Bekešová, S., Komis, G., Křenek, P., Vyplelová, P., Ovečka, M., Luptovčíak, I., Illés, P. et al. (2015) Monitoring protein phosphorylation by acrylamide pendant Phos-Tag™ in various plants. *Front. Plant Sci.* **6**, 336.

Bian, X.H., Li, W., Niu, C.F., Wei, W., Hu, Y., Han, J.Q., Lu, X. et al. (2020) A class B heat shock factor selected for during soybean domestication contributes to salt tolerance by promoting flavonoid biosynthesis. *New Phytol.* **225**, 268–283.

Cao, Y.B., Liang, X.Y., Yin, P., Zhang, M. and Jiang, C.F. (2019) A domestication-associated reduction in K⁺-preferring HKT transporter activity underlies maize shoot K⁺ accumulation and salt tolerance. *New Phytol.* **222**, 301–317.

Cuellar, T., Azeem, F., Andrianteranagna, M., Pascaud, F., Verdeil, J.L., Sentenac, H., Zimmermann, S. et al. (2013) Potassium transport in developing fleshy fruits: the grapevine inward K(+) channel VvK1.2 is activated by CIPK-CBL complexes and induced in ripening berry flesh cells. *Plant J.* **73**, 1006–1018.

Dong, Q., Wallrad, L., Almutairi, B.O. and Kudla, J. (2022) Ca²⁺ signaling in plant responses to abiotic stresses. *J. Integr. Plant Biol.* **64**, 287–300.

Feng, C., He, C.M., Wang, Y.F., Xu, H.H., Xu, K.H., Zhao, Y., Yao, B.W. et al. (2021) Genome-wide identification of soybean Shaker K⁺ channel gene family and functional characterization of GmAKT1 in transgenic Arabidopsis thaliana under salt and drought stress. *J. Plant Physiol.* **266**, 153529.

Fuchs, I., Stölzle, S., Ivashikina, N. and Hedrich, R. (2005) Rice K⁺ uptake channel OsAKT1 is sensitive to salt stress. *Planta* **221**, 212–221.

Gao, Q.F., Gu, L.L., Wang, H.Q., Fei, C.F., Fang, X., Hussain, J., Sun, S.J. et al. (2016) Cyclic nucleotide-gated channel 18 is an essential Ca²⁺ channel in pollen tube tips for pollen tube guidance to ovules in Arabidopsis. *Proc. Natl. Acad. Sci. U. S. A.* **113**, 3096–3101.

Gong, D.M., Guo, Y., Jagendorf, A. and Zhu, J.K. (2002) Biochemical characterization of the Arabidopsis protein kinase SOS2 that functions in salt tolerance. *Plant Physiol.* **130**, 256–264.

Graham, P.H. and Vance, C.P. (2003) Legumes: importance and constraints to greater use. *Plant Physiol.* **131**, 872–877.

Han, W., Ji, Y., Wu, W., Cheng, J.K., Feng, H.Q. and Wang, Y. (2021) ZMK1 is involved in K⁺ uptake and regulated by protein kinase ZmCIPK23 in Zea mays. *Front. Plant Sci.* **12**, 517742.

Hickey, L.T., Hafeez, A., Robinson, H., Jackson, S.A., Leal-Bertioli, S.C.M., Tester, M., Gao, C. et al. (2019) Breeding crops to feed 10 billion. *Nat. Biotechnol.* **37**, 744–754.

Ismail, A.M. and Horie, T. (2017) Genomics, physiology, and molecular breeding approaches for improving salt tolerance. *Annu. Rev. Plant Biol.* **68**, 405–434.

Jia, Q., Li, M.W., Zheng, C., Xu, Y., Sun, S., Li, Z., Wong, F.L. et al. (2021) The soybean plasma membrane-localized cation/H⁺ exchanger GmCHX20a plays a negative role under salt stress. *Physiol. Plant.* **171**, 714–727.

Jin, J.B., Kim, Y.A., Kim, S.J., Lee, S.H., Kim, D.H., Cheong, G.W. and Hwang, I. (2001) A new dynamin-like protein, ADL6, is involved in trafficking from the trans-Golgi network to the central vacuole in Arabidopsis. *Plant Cell* **13**, 1511–1526.

Kereszt, A., Li, D., Indrasumunar, A., Nguyen, C.D., Nontachaiyapoom, S., Kinkema, M. and Gresshoff, P.M. (2007) Agrobacterium rhizogenes-mediated transformation of soybean to study root biology. *Nat. Protoc.* **2**, 948–952.

Kiegle, E., Moore, C.A., Haseloff, J., Tester, M.A. and Knight, M.R. (2000) Cell-type-specific calcium responses to drought, salt and cold in the Arabidopsis root. *Plant J.* **23**, 267–278.

Lara, A., Ródenas, R., Andrés, Z., Martínez, V., Quintero, F.J., Nieves-Cordones, M., Botella, M.A. et al. (2020) Arabidopsis K⁺ transporter HAK5-mediated high-affinity root K⁺ uptake is regulated by protein kinases CIPK1 and CIPK9. *J. Exp. Bot.* **71**, 5053–5060.

Lee, S.C., Lan, W.Z., Kim, B.G., Li, L., Cheong, Y.H., Pandey, G.K., Lu, G. et al. (2007) A protein phosphorylation/dephosphorylation network regulates a plant potassium channel. *Proc. Natl. Acad. Sci. U. S. A.* **104**, 15959–15964.

Li, J., Long, Y., Qi, G.N., Li, J., Xu, Z.J., Wu, W.H. and Wang, Y. (2014) The Os-AKT1 channel is critical for K⁺ uptake in rice roots and is modulated by the rice CBL1-CIPK23 complex. *Plant Cell* **26**, 3387–3402.

Li, W.H., Xu, G.H., Alli, A. and Yu, L. (2018) Plant HAK/KUP/KT K⁺ transporters: function and regulation. *Semin. Cell Dev. Biol.* **74**, 133–141.

Li, J., Gao, Z., Zhou, L., Li, L.Z., Zhang, J.H., Liu, Y. and Chen, H.Y. (2019) Comparative transcriptome analysis reveals K⁺ transporter gene contributing to salt tolerance in eggplant. *BMC Plant Biol.* **19**, 67.

Li, J.F., Shen, L.K., Han, X.L., He, G.F., Fan, W.X., Li, Y., Yang, S.P. et al. (2023) Phosphatidic acid-regulated SOS2 controls sodium and potassium homeostasis in Arabidopsis under salt stress. *EMBO J.* **42**, e112401.

Liang, X.Y., Li, J.F., Yang, Y.Q., Jiang, C.F. and Guo, Y. (2024) Designing salt stress-resilient crops: current progress and future challenges. *J. Integr. Plant Biol.* **66**, 303–329.

Luan, S., Kudla, J., Rodriguez-Concepcion, M., Yalovsky, S. and Gruissem, W. (2002) Calmodulins and calcineurin B-like proteins: calcium sensors for specific signal response coupling in plants. *Plant Cell* **14**, S389–S400.

Ma, Q., Hu, J., Zhou, X.R., Yuan, H.J., Kumar, T., Luan, S. and Wang, S.M. (2017) ZxAKT1 is essential for K⁺ uptake and K⁺/Na⁺ homeostasis in the succulent xerophyte *zygophyllum xanthoxylum*. *Plant J.* **90**, 48–60.

Ma, L., Ye, J.M., Yang, Y.Q., Lin, H.X., Yue, L.L., Luo, J., Long, Y. et al. (2019) The SOS2-SCaBP8 complex generates and fine-tunes an AtANN4-dependent calcium signature under salt stress. *Dev. Cell* **48**, 697–709.

Mao, G.H., Meng, X.Z., Liu, Y.D., Zheng, Z.Y., Chen, Z.X. and Zhang, S. (2011) Phosphorylation of a WRKY transcription factor by two pathogen-responsive

- MAPKs drives phytoalexin biosynthesis in Arabidopsis. *Plant Cell* **23**, 1639–1653.
- Mao, J., Mo, Z., Yuan, G., Xiang, H., Visser, R.G.F., Bai, Y., Liu, H. et al. (2023) The CBL-CIPK network is involved in the physiological crosstalk between plant growth and stress adaptation. *Plant Cell Environ.* **46**, 3012–3022.
- Mohanta, T.K., Yadav, D., Khan, A.L., Hashem, A., Abd Allah, E.F. and Al-Harrasi, A. (2019) Molecular players of EF-hand containing calcium signaling event in plants. *Int. J. Mol. Sci.* **20**, 1476.
- Nieves-Cordones, M., Amo, J., Hurtado-Navarro, L., Martínez-Martínez, A., Martínez, V. and Rubio, F. (2023) Inhibition of SISKOR by SICIPK23-SICBL1/9 uncovers CIPK-CBL-target network rewiring in land plants. *New Phytol.* **238**, 2495–2511.
- Pantoja, O. (2021) Recent Advances in the physiology of ion channels in plants. *Annu. Rev. Plant Biol.* **72**, 463–495.
- Phang, T.H., Shao, G. and Lam, H.M. (2008) Salt tolerance in soybean. *J. Integr. Plant Biol.* **50**, 1196–1212.
- Qiu, Q.S., Guo, Y., Dietrich, M.A., Schumaker, K.S. and Zhu, J.K. (2002) Regulation of SOS1, a plasma membrane Na^+/H^+ exchanger in Arabidopsis thaliana, by SOS2 and SOS3. *Proc. Natl. Acad. Sci. U. S. A.* **99**, 8436–8441.
- Quintero, F.J., Martínez-Atienza, J., Villalta, I., Jiang, X., Kim, W.Y., Ali, Z., Fujii, H. et al. (2011) Activation of the plasma membrane Na/H antiporter Salt-Overly-Sensitive 1 (SOS1) by phosphorylation of an auto-inhibitory C-terminal domain. *Proc. Natl. Acad. Sci. U. S. A.* **108**, 2611–2616.
- Roy, S.J., Negrão, S. and Tester, M. (2014) Salt resistant crop plants. *Curr. Opin. Biotechnol.* **26**, 115–124.
- Rubio, F., Nieves-Cordones, M., Horie, T. and Shabala, S. (2019) Doing 'business as usual' comes with a cost: evaluating energy cost of maintaining plant intracellular K^+ homeostasis under saline conditions. *New Phytol.* **225**, 1097–1104.
- Shen, Y., Shen, L.K., Shen, Z.X., Jing, W., Ge, H.L., Zhao, J.Z. and Zhang, W.H. (2015) The potassium transporter OshAK21 functions in the maintenance of ion homeostasis and tolerance to salt stress in rice. *Plant Cell Environ.* **38**, 2766–2779.
- Steinhorst, L., He, G., Moore, L.K., Schültke, S., Schmitz-Thom, I., Cao, Y., Hashimoto, K. et al. (2022) A Ca^{2+} -sensor switch for tolerance to elevated salt stress in Arabidopsis. *Dev. Cell* **57**, 2081–2094.e7.
- Sun, T.J., Fan, L., Yang, J., Cao, R.Z., Yang, C.Y., Zhang, J. and Wang, D.M. (2019) A Glycine max sodium/hydrogen exchanger enhances salt tolerance through maintaining higher Na^+ efflux rate and K^+/Na^+ ratio in Arabidopsis. *BMC Plant Biol.* **19**, 469.
- Tang, R.J., Wang, C., Li, K. and Luan, S. (2020) The CBL-CIPK Calcium Signaling Network: Unified Paradigm from 20 Years of Discoveries. *Trends Plant Sci.* **25**, 604–617.
- Thiruppathi, D. (2020) Molecular snapshots of the AKT1-CIPK23 complex involved in K^+ uptake. *Plant Physiol.* **182**, 1814–1815.
- Van Zelm, E., Zhang, Y. and Testerink, C. (2020) Salt Tolerance Mechanisms of Plants. *Annu. Rev. Plant Biol.* **71**, 403–433.
- Waadt, R., Schmidt, L.K., Lohse, M., Hashimoto, K., Bock, R. and Kudla, J. (2008) Multicolor bimolecular fluorescence complementation reveals simultaneous formation of alternative CBL/CIPK complexes in plants. *Plant J.* **56**, 505–516.
- Wang, Z., Hong, Y., Zhu, G., Li, Y., Niu, Q., Yao, J., Hua, K. et al. (2020) Loss of salt tolerance during tomato domestication conferred by variation in a Na^+/K^+ transporter. *EMBO J.* **39**, e103256.
- Wu, H.H., Zhang, X.C., Giraldo, J.P. and Shabala, S. (2018) It is not all about sodium: revealing tissue specificity and signalling roles of potassium in plant responses to salt stress. *Plant and Soil* **431**, 1–17.
- Xu, J., Li, H.D., Chen, L.Q., Wang, Y., Liu, L.L., He, L. and Wu, W.H. (2006) A protein kinase, interacting with two calcineurin B-like proteins, regulates K^+ transporter AKT1 in Arabidopsis. *Cell* **125**, 1347–1360.
- Yang, Y.Q. and Guo, Y. (2018) Unraveling salt stress signaling in plants. *J. Integr. Plant Biol.* **60**, 796–804.
- Yin, X.C., Xia, Y.Q., Xie, Q., Cao, Y.X., Wang, Z.Y., Hao, G.P., Song, J. et al. (2020) The protein kinase complex CBL10-CIPK8-SOS1 functions in Arabidopsis to regulate salt tolerance. *J. Exp. Bot.* **71**, 1801–1814.
- You, Z., Guo, S.Y., Li, Q., Fang, Y.J., Huang, P.P., Ju, C.F. and Wang, C. (2023) The CBL1/9-CIPK1 calcium sensor negatively regulates drought stress by phosphorylating the PYLs ABA receptor. *Nat. Commun.* **14**, 5886.
- Zhang, H., Feng, H., Zhang, J., Ge, R., Zhang, L., Wang, Y., Li, L. et al. (2020) Emerging crosstalk between two signaling pathways coordinates K^+ and Na^+ homeostasis in the halophyte *Hordeum brevisubulatum*. *J. Exp. Bot.* **71**, 4345–4358.
- Zhang, M.H., Cao, J.F., Zhang, T.X., Xu, T., Yang, L.Y., Li, X.Y., Ji, F.D. et al. (2021) A Putative Plasma Membrane Na^+/H^+ Antiporter GmSOS1 Is Critical for Salt Stress Tolerance in Glycine max. *Front. Plant Sci.* **13**, 870695.
- Zhao, L., Li, M.M., Xu, C.J., Yang, X., Li, D.M., Zhao, X., Wang, K. et al. (2018) Natural variation in GmGBP1 promoter affects photoperiod control of flowering time and maturity in soybean. *Plant J.* **96**, 147–162.
- Zhu, J.K. (2002) Salt and drought stress signal transduction in plants. *Annu. Rev. Plant Biol.* **53**, 247–273.
- Zhu, J.K. (2016) Abiotic stress signaling and responses in plants. *Cell* **167**, 313–324.

Supporting information

Additional supporting information may be found online in the Supporting Information section at the end of the article.

Figure S1 The identification of genetically modified soybean lines. (a) The relative *GmAKT1* expression in leaves of WT and *GmAKT1-OE* transgenic lines. Data are the mean \pm SD of three independent experiments. Different letters indicate statistically significant differences at $P < 0.05$ by one-way ANOVA. (b, c) The identification of *GmAKT1-KO* soybean lines. Yellow box, blue box and black lines represent untranslated regions (5'UTR and 3'UTR), exons and introns, respectively. Sanger sequencing for identification of *GmAKT1* edited (insertion or deletion) sites around PAM regions.

Figure S2 Genome-wide identification of *GmCIPKs* gene, four expression levels under salt stress and detection of interaction intensity. (a) Phylogenetic relationships of CIPK family members in soybean and Arabidopsis. The phylogenetic tree was constructed using the neighbour-joining method with 1000 bootstrap replicates. The purple circle and yellow triangle represent soybean and Arabidopsis, respectively. (b) Expression analysis of *GmCIPK4*, *GmCIPK6*, *GmCIPK14* and *GmCIPK23* in soybean roots and leaves under salt stress at indicated time points. Different letters represent significant differences ($P < 0.05$, one-way ANOVA). (c) β -Gal activity of *GmAKT1-GmCIPKs* interactions was quantitatively determined in the yeast. Three independent experiments were done with similar results.

Figure S3 Alignments of the amino acid sequences of AKT1 in Arabidopsis and soybean. Alignment was conducted using ClustalW software, and the phosphorylation site of *GmAKT1* is 730 Ser amino acid.

Figure S4 Genome wide identification, expression levels analysis of *GmCBL* family members and detection of interaction strength. (a) Phylogenetic four of *GmCBL* proteins of soybean and Arabidopsis. The tree was derived by the neighbour joining (NJ) with 1000 bootstrap replicates. (b) The expression levels of *GmCBL* family members in soybean roots and leaves under normal and salt stress (120 mM NaCl). (c) *GmCIPK6-GmCBLs* interaction quantitatively determined by the detection of β -Gal activity in the yeast cells. Three biological replicates have similar results.

Figure S5 Subcellular localization of *GmCBL9*, *GmCIPK6* and *GmAKT1* proteins *GmCBL9-GFP*, *GmCIPK6-GFP* and *GmAKT1-GFP* fusion proteins were expressed in Arabidopsis mesophyll protoplasts, respectively. PM-RFP as a cell membrane marker and Nucleus-RFP as a nucleus. The signals of GFP fluorescence were observed in tobacco leaves using confocal (Bar= 10 μm).

Figure S6 *GmCBL9* and *GmCIPK6* enhance salt tolerance in yeast and soybean. (a) Phenotypic analysis of yeast expressing *GmCBL9* or *GmCIPK6* under normal and salt stress. (b) Phenotype of transgenic hair roots of soybean overexpressing *GmCBL9* or *GmCIPK6* under normal and 150 mM NaCl salt-stress conditions for 15 days. (c–h) The values of Na^+ (c, d), K^+ (e, f) and Na^+/K^+

ratio (g, h) of roots were shown in different soybean plants. Asterisks indicate a statistically significant difference in mean expression levels between the control and transgenic hairy roots of soybean (***, $P < 0.01$).

Table S1 Primers used in this paper.